Antiviral Research 85 (2010) 470–481

Contents lists available at ScienceDirect

Antiviral Research

journal homepage: www.elsevier.com/locate/antiviral

Evaluation of the role of three candidate human kinases in the conversion of the hepatitis C virus inhibitor 2′-*C*-methyl-cytidine to its 5′-monophosphate metabolite

Nina L. Golitsina*, Francis T. Danehy Jr., Ross Fellows[1], Erika Cretton-Scott[2], David N. Standring

Idenix Pharmaceuticals, Inc., 60 Hampshire Street, Cambridge, MA 02139, USA

ARTICLE INFO

Article history:
Received 10 March 2009
Received in revised form 20 October 2009
Accepted 21 October 2009

Keywords:
Antiviral drugs
siRNA
Nucleoside/nucleotide derivatives
Metabolism and activation
Uridine–cytidine kinase
Deoxycytidine kinase

ABSTRACT

Nucleoside analogs are effective inhibitors of the hepatitis C virus (HCV) in the clinical setting. One such molecule, 2′-*C*-methyl-cytidine (2′-MeC), entered clinical development as NM283, a valine ester prodrug form of 2′-MeC possessing improved oral bioavailability. To be active against HCV, 2′-MeC must be converted to 2′-MeC triphosphate which inhibits NS5B, the HCV RNA-dependent RNA polymerase. Conversion of 2′-MeC to 2′-MeC monophosphate is the first step in 2′-MeC triphosphate production and is thought to be the rate-limiting step. Here we investigate which of three possible enzymes, deoxycytidine kinase (dCK), uridine–cytidine kinase 1 (UCK1), or uridine–cytidine kinase 2 (UCK2), mediate this first phosphorylation step. Purified recombinant enzymes UCK2 and dCK, but not UCK1, could phosphorylate 2′-MeC in vitro. However, siRNA knockdown experiments in three human cell lines (HeLa, Huh7 and HepG2) defined UCK2 and not dCK as the key kinase for the formation of 2′-MeC monophosphate in cultured human cells. These results underscore the importance of confirming enzymatic kinase data with appropriate cell-based assays. Finally, we present data suggesting that inefficient phosphorylation by UCK2 likely limits the antiviral activity of 2′-MeC against HCV. This paves the way for the use of a nucleotide prodrug approach to overcome this limitation.

1. Introduction

Chronic hepatitis C virus (HCV) infection is thought to affect approximately 170 million individuals worldwide, and it can cause cirrhosis of the liver and hepatocellular carcinoma. The standard therapy for treating chronic HCV is a combination of pegylated interferon (IFN) and ribavirin; however, this therapy is not effective in all patients and is associated with significant side effects. Less than 50% of patients infected with HCV genotype 1, the most common HCV genotype in the United States and Europe, benefit from IFN/ribavirin therapy (Pawlotsky et al., 2007). In recent years a substantial effort has been made to develop new inhibitors for HCV. These molecules target various steps of the viral life cycle, including viral entry, HCV RNA translation, post-translational processing, HCV replication, and virus assembly or release (Pawlotsky et al., 2007).

The HCV RNA-dependent RNA polymerase, NS5B, functions in viral replication and is a highly pursued target. Drugs targeting NS5B are divided into two classes: non-nucleoside analogs, which bind to allosteric sites on the enzyme and inhibit RNA synthesis initiation and/or elongation (Liu et al., 2006; Cooper et al., 2007), and nucleoside analogs, which bind to the enzyme's active site and typically cause termination of viral RNA synthesis (De Francesco and Carfí, 2007). Prodrug forms of several NS5B nucleoside inhibitors have advanced into HCV clinical trials. The underlying nucleoside analogs include 2′-*C*-methyl-cytidine or 2′-MeC (Standring et al., 2003), 2′-fluoro, 2′-methyl-cytidine or 2′-F-2′-MeC (Ali et al., 2008; Reddy et al., 2007; Lalezari et al., 2008) and 4′-azido cytidine or 4′-azidoC (Nelson et al., 2008). However, the utility of drugs targeting NS5B has been somewhat limited by various factors such as toxicity, the need for high doses of drug and rapid development of resistance or lack of efficacy (Meanwell and Koszalka, 2008). While HCV nucleosides appear to have a favorable resistance profile (Le Pogam et al., 2008), the cytosine analogs currently in clinical trials must be given at high doses to elicit potent antiviral effects in the clinic.

In this study, we sought to further investigate factors influencing the efficacy of the cytidine nucleoside analog 2′-MeC. NM283 is a prodrug form of 2′-MeC that was shown to inhibit HCV replication in HCV-infected chimpanzees (Standring et al.,

* Corresponding author. Tel.: +1 617 995 9800; fax: +1 617 995 9801.
E-mail address: golistina.nina@idenix.com (N.L. Golitsina).
[1] Present address: Centocor Discovery Research, 3210 Merryfield Row, San Diego, CA, USA.
[2] Present address: McWhorter School of Pharmacy, Samford University, 800 Lakeshore Drive, Birmingham, AL, USA.

0166-3542/$ – see front matter © 2009 Elsevier B.V. All rights reserved.
doi:10.1016/j.antiviral.2009.10.020

2003) and in humans (Poordad et al., 2007), but was subsequently discontinued. 2′-MeC, like other nucleoside analog inhibitors of NS5B, must be converted into a 5′-triphosphate derivative to be active.

The aim of this study was to identify the kinase or kinases responsible for the first step of 2′-MeC phosphorylation, the conversion of 2′-MeC to the 5′-monophosphate form of 2′-MeC (2′-MeCMP). This first phosphorylation step is inefficient as suggested by recent data (Cretton-Scott et al., 2008; Standring et al., 2008). The resulting low levels of 2′-MeCMP may restrict the subsequent intracellular production of 2′-MeC triphosphate (2′-MeCTP), which in turn limits the antiviral potency of this agent in humans.

The kinases most likely to contribute to the initial phosphorylation of 2′-MeC include two uridine–cytidine kinases (UCKs), UCK1 and UCK2, that participate in the first and rate-limiting step of the pyrimidine-nucleotide salvage pathway in mammalian cells (Anderson and Brockman, 1964; Van Rompay et al., 2003), and deoxycytidine kinase (dCK), which also participates in the pyrimidine salvage pathway, primarily by phosphorylating deoxynucleotides (Van Rompay et al., 2003). In addition to their natural substrates, UCK and dCK kinases have been shown to phosphorylate a variety of nucleoside analogs (Beauséjour et al., 2002; Van Rompay et al., 2001). UCK1 and UCK2 have been shown to phosphorylate a range of uridine and cytidine analogs but are not thought to phosphorylate deoxyribonucleosides or purine ribonucleosides. Despite being closely related at the amino acid sequence level (~72% similarity), the UCK enzymes differ in their substrate specificities (Van Rompay et al., 2001). In addition to its natural substrates deoxycytidine, deoxyadenosine, and deoxyguanosine, dCK has been shown to phosphorylate a broad range of nucleoside analogs (Johansson et al., 1997). There is a controversy in the literature around the enzyme responsible for the phosphorylation of 2′-MeC. Klumpp et al. (2008) reported that 2′-MeC is a substrate for UCK1, not for dCK and UCK2. In contrast Murakami et al. (2007) showed that UCK1 does not phosphorylate 2′-MeC, but found that dCK phosphorylates cytidine and 2′-MeC in vitro, albeit with low efficiency.

In the present study, we used two different strategies to address this issue and investigate the contribution of UCK1, UCK2, and dCK to the in vitro phosphorylation of 2′-MeC. The first evaluated the phosphorylation of 2′-MeC by purified human recombinant kinases, the second examined the effect of depleting the expression of each kinase in cell culture with a gene-specific siRNA. We found that both UCK2 and dCK could phosphorylate 2′-MeC in vitro, but in cell culture experiments, UCK2 was the main kinase responsible for the phosphorylation of 2′-MeC.

2. Materials and methods

2.1. Nucleoside and nucleoside analogs

2′-*C*-methyl-cytidine (2′-MeC), β-L-2′-deoxycytidine (LdC), β-D-2′-deoxy-2′-fluoro-2′-*C*-methyl-cytidine (2′-F-2′-MeC) and their corresponding triphosphates were synthesized at Idenix Pharmaceuticals, Inc. The remaining ribonucleosides, deoxynucleosides and nucleoside analogs, 2′,3′-dideoxycytidine (ddC), cytosine β-D-arabinofuranoside (AraC), 5-iodouridine (5-IodoU), 6-azauridine (6-AzaU), 5-fluorocytidine (5-FC) and 2-chloro-2′-deoxyadenosine (CdA) were obtained from Sigma–Aldrich (St. Louis, MO) or ICN Biomedicals (Costa Mesa, CA). [6-^{3}H]-2′-dC (9 Ci/mmol), [5-^{3}H(N)]-C (24.8 Ci/mmol), [5,6-^{3}H]-U (34.5 Ci/mmol), 2′-MeC (11.7 Ci/mmol) and 2′-F-2′-MeC (8.5 Ci/mmol), were obtained from Moravek Biochemicals (Brea, CA). The structures of these compounds are shown in Fig. 1.

2.2. Cloning and expression

cDNA clones containing gene NM_031432 or gene NM_012474, for UCK1 and UCK2, respectively, were obtained from OriGene (Rockville, MD). Full-length human UCK1 (encoding a 277 amino acid protein of 31 kDa) and UCK2 (encoding a 261 amino acid protein of 29 kDa) were amplified by PCR with primers containing NdeI and XhoI restriction enzyme sites. UCK1 primers were (from 5′ to 3′) ACATATGGCTTCGGCGGGAGGCG and CTCTCGAGTCAGTGGGGTCTGCTGCTGGA; UCK2 primers were (from 5′ to 3′) AACATATGGCCGGGGACAGCGAGCAG and CTCTCGAGTCAATGCGGCCTGCTGCTGGA. The PCR-amplified fragments were cloned at a 5′-NdeI and 3′-XhoI sites into the pET-15b vector (EMD Biosciences, Madison, WI), that contains an N-terminal His-tag. A cDNA clone for the dCK gene NM_000788.1 was obtained from Invitrogen (Carlsbad, CA) and sub-cloned into the pDEST17 expression vector with an N-terminal His-tag (Invitrogen, Carlsbad, CA). The expression plasmids were sequenced (Tufts University, Boston, MA) to confirm the correct full-length gene sequences. Expression plasmids with UCK1 or UCK2 were transformed into the *Escherichia coli* strain BL21 (DE3) (Invitrogen, Carlsbad, CA) and dCK into *E. coli* BL21-AI™ (Invitrogen, Carlsbad, CA) competent cells. Five milliliters of overnight culture grown from a single transformed colony were added to 500 mL of fresh LB medium supplemented with 100 μg/mL carbenicillin and grown at 37 °C. Protein expression was induced at cell density OD_{600} = 0.8 (UCK1 and UCK2) or at a cell density of OD_{600} = 0.5 or 0.6 (dCK) by addition of isopropyl-beta-D-thiogalactopyranoside (IPTG) to a final concentration of 1 mM (UCK1 or UCK2) or arabinose to a final concentration of 0.02% (dCK). The bacteria were cultured for 4 h at 22 °C (UCK1 and UCK2) or 37 °C (dCK), then harvested by centrifugation at 5000 × *g* for 10 min at 4 °C. Bacteria pellets were stored at −80 °C until purification.

2.3. Protein purification

Fifteen milliliters of lysis solution (20 mM Tris–HCl, pH 7.8 for UCK1 or pH 7.4 for UCK2 and dCK, 500 mM NaCl, 40 mM imidazole, 1× BugBuster solution [Novagen, Madison, WI], 1× ethylenediaminetetraacetic acid [EDTA] free complete protease inhibitor [Roche Applied Sciences, Indianapolis, IL], 10% glycerol, 37.5 U/mL benzonase, 2 mM dithiothreitol [DTT]) were added per gram of wet cell paste. The resuspended cell paste was incubated with 10,000 U/mL of lysozyme solution (EMD Chemicals, Gibbstown, NJ) for 20 min at room temperature (RT) with gentle shaking. The lysate was clarified at 19,000 × *g* for 1 h at 4 °C.

All purifications were performed on an AKTA Purifier (GE Healthcare, Piscataway, NJ). For UCK1 and UCK2, clarified lysate was loaded on a 1 mL HisTrap HP column (GE Healthcare, Piscataway, NJ) equilibrated with 10 column volumes (CV) of buffer A (20 mM Tris–HCl, pH 7.8 for UCK1 or pH 7.4 for UCK2, 500 mM NaCl, 10% glycerol, 2 mM DTT, 0.4 mM Pefabloc SC [Roche Applied Sciences, Indianapolis, IL], 0.1% Triton X-100 [Calbiochem, San Diego, CA]) substituted with 8% buffer B (same as buffer A without Triton X-100 and with 500 mM imidazole at 0.5 mL/min). For dCK, lysate was loaded on a 5 mL HisTrap HP column equilibrated with the buffer A at pH 7.4 substituted with 1.0% buffer B at 2.0 mL/min. Unbound proteins were removed by 20 CV of 8% Buffer B. Two step gradient washes with 10% and 20% buffer B, 20 CV each, removed non-specifically bound *E. coli* proteins. His-tagged proteins were eluted by a linear gradient (20–100% buffer B, 20 CV). One milliliter (UCK1 and UCK2) or 5 mL (dCK) fractions were collected and analyzed by sodium dodecyl sulfate polyacrylamide gel electrophoresis (SDS PAGE) followed by staining with InVision His-Tag In-gel (Invitrogen, Carlsbad, CA) and GelCode Blue Stain Reagent (Pierce Biotechnology, Rockford, IL). Fractions containing

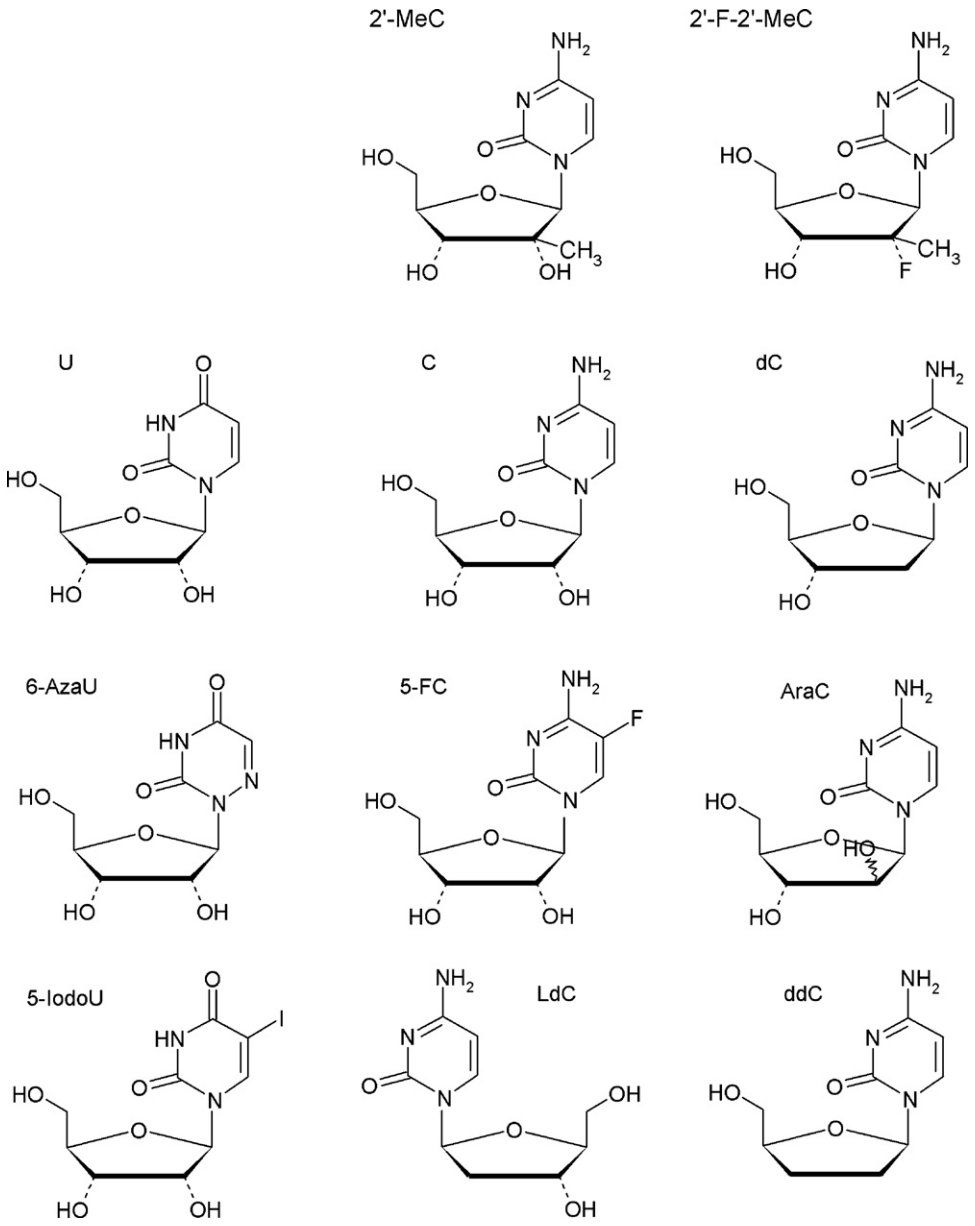

Fig. 1. Nucleoside and nucleoside analogs structures.

pure His-tagged kinase were combined and buffer exchanged on PD10 columns (GE Healthcare, Piscataway, NJ) equilibrated at 4 °C with 50 mM Tris pH 7.8, 100 mM NaCl, 20% glycerol, 10 mM DTT and 0.4 mM pefabloc. After clarification for 20 min at 16,000 × *g* at 4 °C, protein concentration was measured using Coomassie Plus (Pierce Biotechnology, Rockford, IL). Bovine serum albumin (BSA) (New England BioLabs, Beverly, MA), was added to a concentration of 0.5 mg/mL and proteins aliquots were stored at −80 °C. The purified proteins were >96% pure as evaluated by SDS PAGE.

The presence of phosphatases in the enzyme preparations was excluded by comparison of the enzyme activity with and without phosphatase inhibitor NaF (5 mM). No changes in the activity were found (data not shown).

The presence of deaminases in the purified enzymes was excluded by HPLC analysis of ^{3}H-2′-MeC after 1 h incubation at 37 °C with dCK, UCK1 or UCK2 in the presence of 2 mM Mg-ATP. HPLC analysis did not reveal the appearance of any 2′-MeU derivatives of NM107.

2.4. Enzyme phosphorylation assay

Phosphorylation assays were performed using fresh aliquots of recombinant UCK1, UCK2 or dCK proteins. The test nucleoside substrates were added at a final concentration of 1 mM in a 50 μL reaction mixture containing 50 mM Tris–HCl, pH 7.6, 5 mM $MgCl_2$, 4 mM unlabeled ATP, 1 μCi of [γ-^{33}P] ATP (3000 Ci/mmol, Amersham Biosciences, Piscataway, NJ), 0.5 mg/mL albumin and 5 ng of enzyme. The reaction mixtures were incubated 30 min at 37 °C, heated at 100 °C for 2 min and centrifuged for 5 min at 16,000 × *g*. Two microliters of the reaction mixtures were spotted on poly(ethylenimine)-cellulose F chromatography sheets (EMD Chemicals, Madison, WI), and the nucleoside monophosphate products were separated by thin-layer chromatography (TLC) in a buffer containing either 0.5 M LiCl or NH_4OH/isobuturic acid/water (1:66:33, v/v). TLC sheets were autoradiographed on a Storm 860 PhosphorImager (Amersham Biosciences, Piscataway, NJ) and quantified using ImageQuant TL v2003.03 (Amersham Biosciences,

Piscataway, NJ). Products were identified using monophosphate reference standards.

Steady-state activity parameters for dCK, UCK1 and UCK2 were measured using a radiochemical method (Ives et al., 1969; Ahmed, 1981) with ATP as a phosphate donor. The assays were performed in a total reaction volume of 0.05 mL in 100 mM Tris–HCl, pH 7.5, 100 mM KCl, 2 mM $MgCl_2$, 2 mM ATP, 5 mM DTT, 0.5 mg/mL BSA and 1 μM [6-^{3}H]-2′-dC (Ci/mmol), or [5-^{3}H(N)]-C (24.8 Ci/mmol), or [5,6-^{3}H]-U (34.5 Ci/mmol), with or without 5 mM NaF. Mg-ATP was increased to 5 mM when ^{3}H-2′-MeC (8.7 Ci/mmol) and ^{3}H-2′-F-2′-MeC (8.5 Ci/mmol) were used. All ^{3}H-labeled substrates were obtained from Moravek Biochemicals (Brea, CA). The amount of enzyme added to the reaction was adjusted so that no more than 20% of the substrate was consumed. After incubation at 37 °C samples were heated at 100 °C for 2 min, placed in ice for 1 min and centrifuged for 5 min at 16,000 × *g* to remove denatured protein. An aliquot of 25 μL from each sample were diluted in 200 μL of water to decrease salt concentration in samples and 50 μL of diluted samples were spotted in triplicate on Whatman DE-81 filters, dried, washed by 1 mM phosphate buffer pH 7.0 as described by Ahmed (1981) and dried again. For loading control 10 μL of each sample was spotted on two filters and dried. DE-81 discs were placed in scintillation vials, eluted with 1 mL 0.2 M NaCl/0.1 M HCl solution for 1 h and were counted in 18 mL of scintillation fluid. Steady-state parameters were determined by using SigmaPlot 2004 Enzyme Kinetics software and Michaelis–Menten equation.

2.5. siRNA transfection

Twelve-well plates were seeded with 1×10^5 cells per well (HeLa and Huh7 cells) or 2×10^5 cells per well (HepG2 cells) in 1 mL of appropriate cell medium. When cells reached ≥50% confluence, the medium was replaced by 800 μL antibiotic-free medium. Transfection agent Lipofectamine™ (LP2000, Invitrogen, Carlsbad, CA) was diluted 100× in Opti-MEM medium (Invitrogen, Carlsbad, CA) and incubated 20 min at RT. The siRNAs were diluted in Opti-MEM medium to 1 pmol/μL, and 100 μL was mixed with 100 μL diluted LP2000. A designated non-targeting siRNA (D001210, Dharmacon, Fisher Scientific, Rockford, IL) provided a control for non-specific siRNA transfection effects on gene expression. For UCK1 silencing, siRNAs HSS130222, HSS130223 and HSS130224 (Invitrogen, Carlsbad, CA) and siRNA ID 1197 (Ambion, Austin, TX) were used. For UCK2 silencing, siRNAs A (ID 893), B (ID 894), and C (ID 895) (Ambion, Austin, TX) were tested. For dCK silencing, the test siRNAs were ID 68, ID 69, and ID 70 (Ambion, Austin, TX). After 1 h incubation at RT, 200 μL of the siRNA/transfection agent mixture were added to each well. The total amount of test siRNA was 100 pmol/well. Plates were incubated at 37 °C/5% CO_2. Each experiment was done at least in triplicate. Protein levels were analyzed by Western blot, as described below, after 24, 48 and 72 h treatment with siRNA.

2.6. Antibodies

UCK1 and UCK2 antisera were generated by Capralogics (Hardwick, MA) (Shimamoto et al., 2002). Briefly, peptides encoding amino acids 259–277 of UCK1 or amino acids 243–261 of UCK2 were separately conjugated to keyhole limpet hemocyanin via a cysteine and injected into New Zealand White rabbits (two rabbits each). Antibodies were purified by standard procedures. For Western blotting, the anti-UCK1 antibody was diluted 1:1000, the anti-UCK2 antibody was diluted 1:5000, and the anti-dCK antibody was diluted 1:500. Glyceraldehyde-3-phosphate dehydrogenase (GAPDH) was detected using a mouse monoclonal antibody (Ambion, Austin, TX) at 1 μg/mL.

2.7. Western blotting

Huh7, HepG2 or HeLa cells were washed twice with 1 mL cold phosphate buffered saline (PBS). Two hundred–300 μL of ice-cold Reportasol (Novogen, Madison, WI) lysis buffer was added directly to each well. Lysates were collected after 10 min incubation at RT, clarified 10 min at 16,000 × *g*, and total protein concentrations were measured with the BCA assay kit (Pierce, Fisher Scientific, Rockford, IL).

Ten micrograms of cell lysate was loaded per lane on a 4–12% gradient NuPage gel (Invitrogen, Carlsbad, CA), run with MES buffer according the manufactures protocol and transferred to a polyvinylidene fluoride (PVDF) membrane (Invitrogen, Carlsbad, CA). The PVDF membrane was stained for 5 min in Ponceau S solution (Mallinkrodt, Hazelwood, MO), de-stained with water until background was gone, and photographed. The membrane was washed in Tris-buffered saline with 0.05% Tween-20 (TBST) at RT until all stain was removed, and placed in 5% milk/1× TBS blocking buffer for at least 1 h at RT. The membrane was then incubated with primary antibody diluted in TBST/1% milk overnight at 4 °C. The blot was washed three times in TBS or TBST and incubated with either goat anti-rabbit-HRP antibody (BioRad, Hercules, CA) or goat anti-mouse IgG-AP (BioRad, Hercules, CA) diluted in TBST and 1% milk for 1 h at RT. The blot was then washed again three times in TBS or TBST. For horseradish peroxidase conjugated antibody, the enhanced chemoluminescence Western blotting detection kit (GE Healthcare, Piscataway, NJ) was used for detection. For alkaline phosphatase (AP) conjugated antibodies, the AP conjugate substrate kit (BioRad, Hercules, CA) was used for detection.

2.8. Determination of the dCK activity in cell lysates

This was performed according to Arner et al. (1992) on aliquots of the lysates prepared as described above in Section 2.7. The protein concentration of the lysate was first adjusted to 1 μg/μL, then 25 μL of cell lysate were added to 25 μL of assay mix consisting of 0.2 mM CdA substrate, 4 mM ATP, 4 μCi ^{33}P-γATP, 4 mM $MgCl_2$, 200 mM NaCl, 20 mM NaF, 4 mM DTT in 100 mM Tris–HCl pH 7.4. After 45 min at 37 °C, 2 μL of the reaction mixtures were spotted on poly(ethylenimine)-cellulose F chromatography sheets (EMD Chemicals, Madison, WI), and the nucleoside monophosphate products were separated and quantified as described in Section 2.4. CdA monophosphate produced by incubating CdA with purified recombinant dCK in the presence of Reportazol provided a chromatography standard, while reactions run without the CdA substrate provided background controls for the TLC. The CdA phosphorylation in lysates from cells treated by siRNA was evaluated as a % of the CdA phosphorylation seen in lysates from untreated control cells.

2.9. HPLC determination of phosphorylation

Some 48 h after addition of siRNA to cells, medium was removed and drug treatment was initiated by adding 1 mL of culture medium containing [^{3}H]-2′-MeC (or other nucleoside) to a final concentration of 10 μM and 1000 dpm/pmol. Drug stock solutions were made up freshly in antibiotic-free assay medium. The final dimethyl sulfoxide concentration was 0.5%. Plates were gently mixed by rocking back and forth and incubated at 37 °C/5% CO_2 for 24 h. After removal of medium, cells were washed three times with cold PBS and extracted with 600 μL 70% methanol (at −20 °C) for at least 24 h at −20 °C. The cell extracts then were harvested, centrifuged to remove cellular debris and dried down under a gentle stream of filtered air. The dried cell extracts were resuspended in 200 μL of water and analyzed by reverse-phase with ion-pairing chromatography using an Agilent model 1100 instrument (Agilent, Santa Clara,

CA). The mobile phase consisted of buffer A (25 mM potassium phosphate, 5 mM tetrabutyl ammonium phosphate (TBAP), pH 6.0) and buffer B (methanol). A multi-stage linear gradient from 0% to 30% buffer B was run from 0 to 60 min according to the following schedule: 10 min – 0% buffer B; 20 min – 20% buffer B; 30 min 20% buffer B; 35 min – 30% buffer B. Radioactivity was analyzed by online detection using a radiomatic 500TR Flow Scintillation Analyzer (Packard/Perkin Elmer Life and Analytical Sciences, Waltham, MA). Each analyte was quantified based on the area of its respective radioactive peak and identified based on its peak elution pattern compared to the elution patterns of cytidine, uridine and their corresponding 5′-phosphate derivatives. Identity was then confirmed by co-elution of the radiolabeled peaks with authentic reference standards. Finally the identity of monophosphate products was further established by digestion of cell extracts with 1–5 units of alkaline phosphatase for 60 min at 37 °C, thereby releasing the parent nucleoside (e.g. 2′-MeC) which was identified as described above.

2.10. Design of siRNA testing strategy and experimental controls

The optimal concentrations of siRNA reagents and the use of single versus multiple siRNAs were evaluated in exploratory experiments. To ensure that all observed silencing was due to a specific effect of the siRNA on its target gene, the negative controls used in each experiment included a transfection reagent that lacked siRNA as well as a commercially available non-targeting siRNA control. Moreover, each gene-specific siRNA reagent served as negative controls for the other two kinase genes.

The effect of the siRNAs on the expression of the specific target kinase was determined in transfected cells by measuring the disappearance of UCK1, UCK2 or dCK proteins by Western blotting. New antibodies specific for each enzyme were developed in conjunction with this study (for details see Section 2.6). These antibodies allowed the specific identification and assessment of UCK1, UCK2 and dCK levels in lysates from each cell line. Equivalent loading of lysates for each transfection experiment was verified by Western blot staining of GAPDH with GAPDH-specific antibodies.

Finally, the impact of each kinase on 2′-MeC or 2′-F-2′-MeC phosphorylation was determined in conjunction with the silencing experiments by HPLC/radiometric quantification of total phosphorylated nucleoside analog species (appearing in cell lysates primarily as the respective triphosphates) recovered from control cells versus silenced cells following exposure to [^{3}H]-labeled drug. The relevant mono-, di- and triphosphate species were identified using synthetic reference standards (see Section 2.9).

3. Results

3.1. Phosphorylation of 2′-MeC by recombinant enzymes in vitro

Two different groups have obtained conflicting results related to enzymes that can phosphorylate 2′-MeC to 2′-MeCMP. Klumpp et al. (2008) reported that dCK and UCK2 do not phosphorylate 2′-MeC and that 2′-MeC is a substrate for UCK1. Murakami et al. (2007), on the other hand, showed that UCK1 does not phosphorylate 2′-MeC. Instead they found that 2′-MeC can be phosphorylated by dCK although with low efficiency.

Our paper sought to resolve this controversy using two different approaches: by testing 2′-MeC phosphorylation with purified kinases and by evaluating the impact of silencing the expression of the specific kinase on 2′-MeC phosphorylation in cell cultures using siRNA technique.

We first evaluated whether the purified recombinant UCK1, UCK2, or dCK enzymes could phosphorylate 2′-MeC and 2′-F-2′-MeC nucleoside analogs in vitro. The structures of the various nucleosides and nucleoside analogs tested in this report are shown in Fig. 1. His-tagged human UCK1, UCK2 and dCK enzymes were each expressed in *E. coli* and purified to greater than 96% homogeneity as shown in Fig. 2.

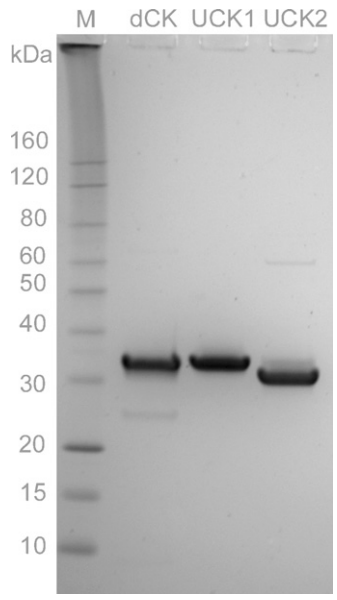

Fig. 2. SDS PAGE of purified recombinant dCK, UCK1 and UCK2 enzymes. M = proteins molecular weight markers.

The steady-state catalytic parameters for recombinant UCK1, UCK2 and dCK, tested in standard DE-81 filter assay with ^{3}H-labeled compounds as described in Section 2, are summarized in Table 1. The purified enzymes had Km and specific activity values similar to those published by other researchers (Van Rompay et al., 2001; Roy et al., 2004; Usova et al., 2004; Murakami et al., 2007).

Purified His-tagged recombinant dCK efficiently phosphorylated dC (Table 1) with a Km of 1.5 ± 0.5 μM, within the range of values reported in the literature (0.13–9 μM) (Shafiee et al., 1998; Sabini et al., 2003; Usova et al., 2004; Roy et al., 2004; Murakami et al., 2007). Consistent with literature reports dCK phosphorylated a wide range of cytidine analogs: AraC, ddC and 5-FC (data not shown). The nucleoside monophosphate products of in vitro phosphorylation reactions were resolved by TLC and their identity was verified using appropriate reference standards and evaluated as described in Section 2. Both 2′-F-2′-MeC and 2′-MeC were phosphorylated by dCK although with low efficiency: 118 and 438 times less than dC, respectively (Table 1).

These data are generally consistent with the findings of Murakami et al. (2007) suggesting that 2′-F-2′-MeC and 2′-MeC are potential, albeit less efficient, substrates for the human dCK enzyme. Our data do not appear to support the finding of Klumpp et al. (2008).

Purified His-tagged recombinant UCK1 efficiently phosphorylated C and U (Table 1) with a Km of 194 ± 127 μM and Km of 452 ± 37 μM for C and U, respectively, consistent with the range of values reported in the literature (131–291 μM and 225–407 μM for C and U, respectively) (Van Rompay et al., 2001; Roy et al., 2004; Murakami et al., 2007). Consistent with a prior report (Van Rompay et al., 2001), purified recombinant UCK1 displayed a relatively restricted substrate profile; it effectively phosphorylated its natural substrates, uridine and cytidine (Table 1), as well as the nucleoside analog 5-IodoU and was less active with 6-AzaU and 5-FC (data not shown). UCK1 did not phosphorylate 2′-MeC and 2′-F-2′-MeC tested at up to 5 mM (Table 1) and LdC (data not shown) in the standard assay. Indeed, no trace of 2′-MeC or 2′-F-2′-MeC

Table 1
Steady-state kinetic parameters for dCK, UCK1 and UCK2 with ATP as a phosphate donor. Kcat was calculated using molecular mass of 33.16, 33.707 and 31.572 kDa for recombinant dCK, UCK1 and UCK2 subunits, respectively. Values are reported as means ± standard deviations of four experiments for dC, C or U, eight experiments for 2′-MeC and two experiments for 2′-F-2′-MeC.

Compound	Km (μM)	Vmax (nmol/min/mg)	kcat (s^{-1})	kcat/Km (s^{-1} M^{-1})	Relative efficiency	Enzyme
dC	1.5 ± 0.5	125 ± 30	0.07	46296	1	dCK
2′-MeC	451 ± 225	87 ± 33	0.048	107	0.0023	
2′-F-2′-MeC	230 ± 74	162 ± 89	0.09	391	0.0084	
C	194 ± 127	544 ± 377	0.31	1598		UCK1
U	452 ± 37	1270 ± 159	0.71	1578		
2′-MeC	NA, 5 mM	NA, 5 mM				
2′-F-2′-MeC	NA, 5 mM	NA, 5 mM				
C	72 ± 21	1975 ± 500	1.03	14306	1	UCK2
U	121 ± 27	49030 ± 12700	1.41	22511	1.6	
2′-MeC	3131 ± 1718	837 ± 496	0.44	139.8	0.0098	
2′-F-2′-MeC	NA, 5 mM	NA, 5 mM				

monophosphates was seen even after prolonged incubation (data not shown) indicating that UCK1 does not utilize 2′-MeC and 2′-F-2′-MeC as a substrates. Our results are in a good agreement with Murakami et al. (2007), and contradict those of Klumpp et al. (2008).

Our purified recombinant UCK2 efficiently phosphorylated C and U (Table 1) with Km values of 72 ± 21 μM and 121 ± 27 μM for C and U, respectively, close to the values reported by Van Rompay et al. (2001) (86 and 50 μM for C and U, respectively) and exhibited a much wider substrate spectrum than UCK1 in accord with the findings of Van Rompay et al. (2001). Thus, UCK2 phosphorylated the analogs 5-HydroxyU, 5-FC and 6-AzaU (data not shown). UCK2 showed no activity against 2′-F-2′-MeC (Table 1). Contrary to Klumpp et al. we found that 2′-MeC is a weak substrate for UCK2 with a Km of 3.1 ± 1.7 mM (Table 1). 2′-MeC was 100× less effective as a substrate in terms of catalytic efficiency (kcat/Km) than C for UCK2 compared to 400× less effective than dC for dCK (Table 1).

In summary, our in vitro biochemical data suggest that the likely candidate enzymes for phosphorylation of 2′-MeC are UCK2 and dCK, and effectively rule out the involvement of UCK1.

3.2. siRNA analysis of the kinases involved in the phosphorylation of 2′-MeC in human cell lines

Since the relative contribution of UCK2 and dCK to phosphorylation of 2′-MeC in the cellular environment likely depends on factors such as the expression level of these enzymes and the competition between 2′-MeC and the natural substrates, we decided to further evaluate the contribution of each of these enzymes in human cell lines. To this end, we used a siRNA approach to specifically target each of the UCK1, UCK2 and dCK kinases. The effect of depleting each enzyme on the extent of phosphorylation of 2′-MeC in cells was used to determine the role of each kinase in the formation of phosphorylated 2′-MeC species.

The inclusion of appropriate controls was an important aspect of the experimental design for the siRNA study (see Section 2). A combination of positive and negative controls was included in every experiment to rule out any misinterpretation of the experimental results.

All findings were verified in three different human cell lines: HeLa cells and two human hepatocyte-derived cell lines (HepG2 hepatocellular liver carcinoma and Huh7 hepatoma cells). Of note, the Huh7 cell line is permissive for the replication of the HCV replicon and is the cell line typically used for the preclinical assessment of HCV antiviral agents. We also note that we attempted to study the kinases in primary human hepatocytes. These experiments did not yield useful information since we were unable to detect UCK2 or dCK by Western blot or get siRNA approaches to work in these cells, which are more difficult to work with than cell lines.

Each kinase gene was silenced without significantly affecting the other two genes using gene-specific siRNA reagents. The effect of the siRNAs on the expression of the specific target kinase was determined in transfected cells by measuring the disappearance of UCK1, UCK2 or dCK proteins by Western blotting.

Finally, the impact of each kinase on 2′-MeC or 2′-F-2′-MeC phosphorylation was determined in conjunction with the silencing experiments by HPLC/radiometric quantification of total phosphorylated nucleoside analog species (primarily the respective triphosphates) recovered from control cells versus silenced cells following exposure to [^{3}H]-labeled drug. The relevant mono-, di- and triphosphate species were identified using synthetic reference standards (see Section 2).

In summary, the use of different siRNA reagents and antibodies, together with the evaluation of phosphorylation of the nucleosides, provided an extensive panel of controls to ensure the correct interpretation of all results.

3.3. Effect of siRNAs on kinase expression

In exploratory experiments, conditions for the most efficient siRNA delivery and gene silencing were tested and optimized in each cell line by measuring the decreased expression of target kinase enzyme by Western blotting. The conditions investigated included cell density, the use of different transfection reagents, the use of different siRNA sequences, the use of single versus combinations of gene-specific siRNAs at different ratios, and finally the time required to achieve a maximum reduction in kinase levels following transfection of the siRNA. Some of these data are shown in Figs. 3 and 4.

As seen in Fig. 3A, immunostaining with a UCK2-specific antibody reveals that the amount of UCK2 decreased substantially in HeLa cells in response to transfection with UCK2-specific siRNAs but not with a control (random) siRNA. Immunostaining with a GAPDH antibody verified that equal amounts of lysates were loaded on this gel, demonstrating that the decrease in UCK2 expression was gene specific. Testing of three different siRNAs singly or in combination, as described in Section 2 (data not shown), established that maximal UCK2 suppression was attained with a 1:1 combination of two siRNAs. As shown in Fig. 3A, the combination of siRNAs B and C, targeting exon 4 (B) and exon 5 (C) of the UCK2 gene, appeared to be slightly superior to the combination of siRNAs A and C and was thus selected for the remaining experiments. Essentially maximal UCK2 protein depletion was achieved by 24 h post-transfection (Fig. 4A) and maintained through 72 h post-transfection (data not shown). Since all three kinases were effectively depleted 48 h post-transfection in response to their respective siRNA reagents (see below), this time frame was routinely used when comparison between the proteins

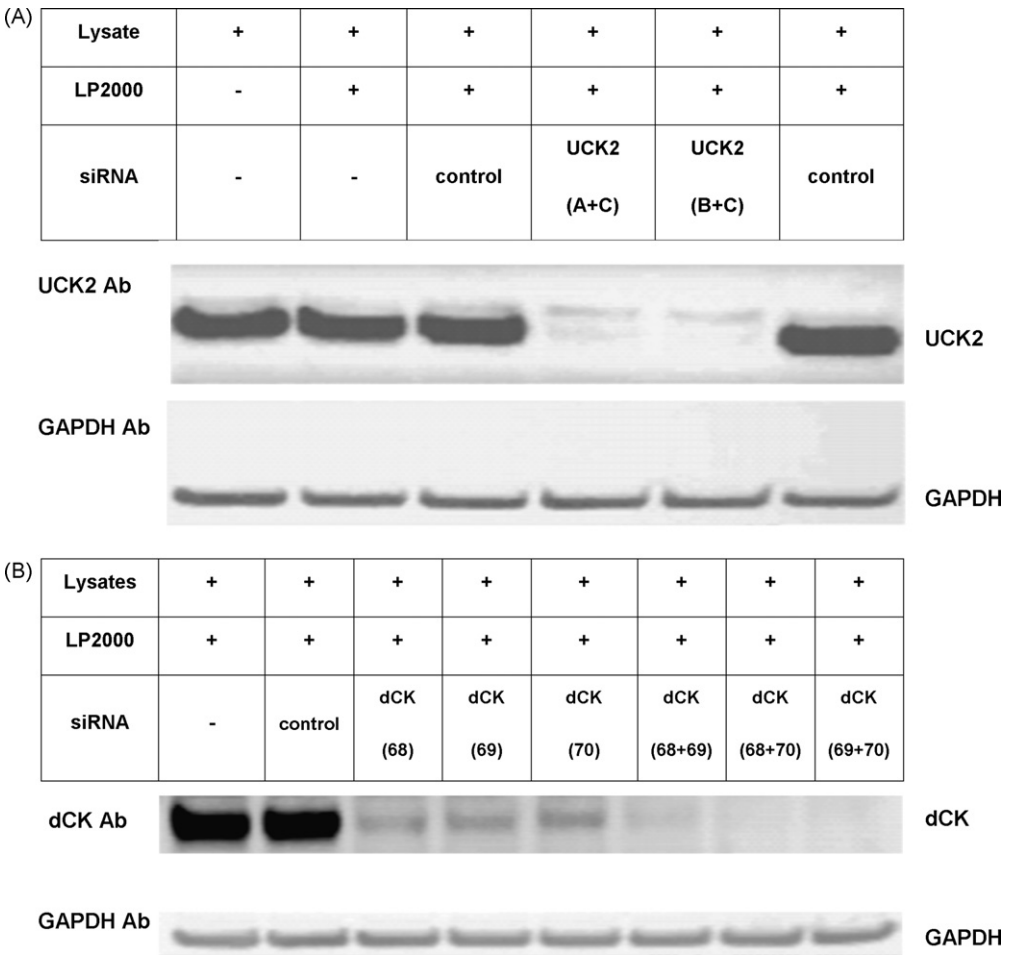

Fig. 3. The effect of incubation with different gene-specific siRNAs on the kinase levels in HeLa cells. (A) Western blot analysis performed with UCK2-specific (top panel) and GAPDH-specific (bottom panel) antibodies. For description of reagents and siRNAs see Sections 2 and 3. (B) Western blot analysis performed with dCK-specific (top panel) and GAPDH-specific (bottom panel) antibodies.

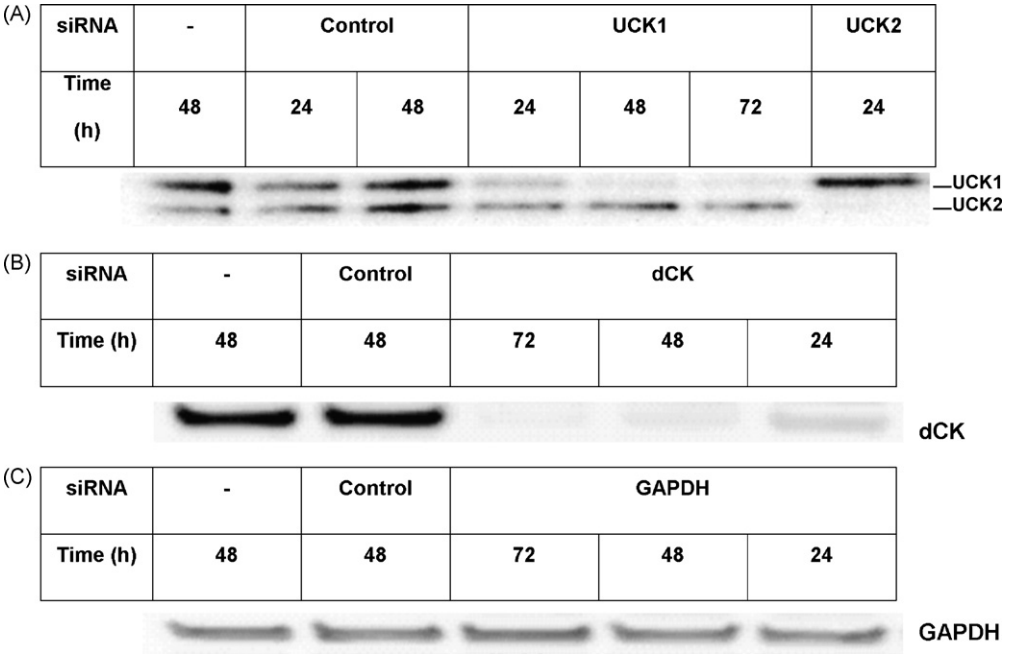

Fig. 4. Effects of incubation time on the depletion of UCK1, UCK2 and dCK in HeLa cells by each gene-specific siRNA. Western blot were stained with antibodies recognizing (A) UCK1 and UCK2, (B) dCK, and (C) GAPDH.

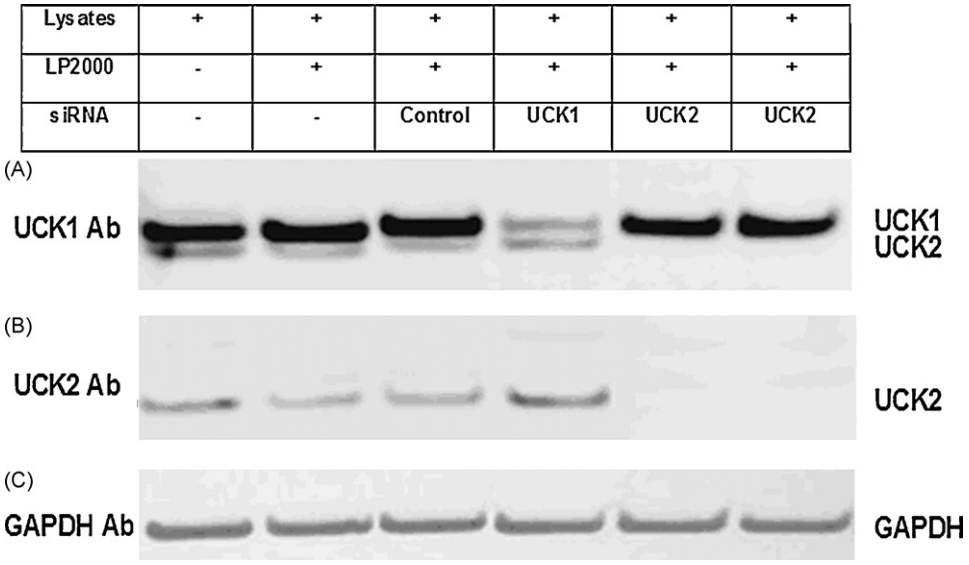

Fig. 5. Silencing of UCK1 and UCK2 expression in HepG2 cells. Western blot immunostained for UCK1 (A), UCK2 (B) and GAPDH (C).

was needed (e.g. for the phosphorylation experiments described below).

For dCK, the Western blot analysis revealed that the amount of kinase protein in HeLa cells was not affected by the control siRNA but decreased significantly in response to transfection with each of the three individual test siRNAs, ID68, ID69 and ID70 (Fig. 3B). Equal protein loading was again verified by GAPDH immunostaining (Fig. 3B). The most efficient suppression was seen with 1:1 combinations of two siRNAs, 68+70 or 69+70, (Fig. 3B). The combination of siRNAs 69+70, targeting exons 2–3 (69) and exon 7 (70) of the dCK gene, gave the most effective silencing and was selected for further studies. Silencing of dCK was evident (Fig. 4B) through 72 h post-transfection and there was good suppression of dCK protein levels at 48 h post-transfection, the time point chosen for subsequent experiments.

For UCK1 silencing, four siRNAs were evaluated singly and in combination and the best results were obtained with a single siRNA, HSS130223 (data not shown). In HeLa cells (Fig. 4A), this siRNA effectively depleted UCK1 protein but not UCK2 protein, as judged by staining with our anti-UCK1 antibody that recognizes both proteins (which are closely related at the amino acid sequence level). Immunostaining for GAPDH again verified the loading of equal amounts of lysates on the gel (Fig. 4C). The time course for UCK1 (Fig. 4A) showed that 48 rather than 24 h was required to achieve effective silencing for this protein. Fig. 5 shows the results obtained in HepG2 cells and compares the staining obtained with the antibody raised against UCK1 protein (Panel A) versus the anti-UCK2 antibody that is specific for UCK2 (Panel B). Both antibodies confirmed that the UCK2-specific siRNA depleted UCK2 protein. Immunostaining with UCK1 antibody demonstrated that HepG2 cells have higher amounts of UCK1 compared to UCK2 than HeLa (Fig. 4A) and Huh7 cells (Fig. 6). The data further confirmed that UCK2 knockdown did not significantly deplete UCK1. Conversely, only the UCK1-specific siRNA depleted UCK1 protein levels. GAPDH

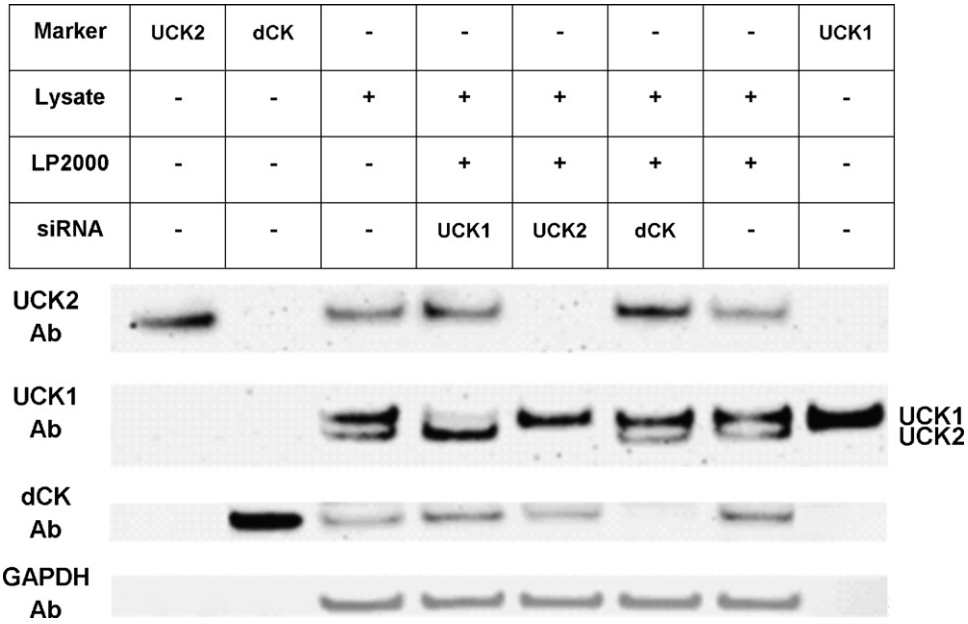

Fig. 6. Gene-specific knockdown of kinase proteins in Huh7 cells. Western blot analysis using siRNA and antibody reagents as indicated on the figure.

staining again verified the loading of equal amounts of lysates on the gel (Fig. 5C).

The experiment shown in Fig. 6 clearly demonstrates that depletion of each of the three kinase proteins could be achieved independent of the other two in Huh7 cells in response to the appropriate siRNA reagent. Similar results in terms of the extent and specificity of silencing were obtained in all three cell lines (data not shown). Importantly, kinase depletion was only observed in response to the correct gene-specific siRNA in all three cell lines and was not seen in cells treated with transfection agent alone or transfected with the non-targeting random siRNA as seen in Figs. 3–6.

3.4. Phosphorylation of 2′-MeC in cells after specific siRNA transfection

Next, we determined how reductions in the levels of UCK1, UCK2, and dCK proteins affected the ability of human cell lines to phosphorylate 2′-MeC and 2′-F-2′-MeC. Cells were transfected with the appropriate siRNA and cultured for a further 48 h to provide extensive depletion of the target kinase protein that was verified by parallel Western blot experiments. The depleted cells were then incubated with the appropriate radiolabeled nucleoside analog for 24 h. The resultant phosphorylated nucleoside products (primarily in the form of triphosphate species as described further below) were then separated by HPLC and quantified (see Section 2 for further details).

The results of these experiments in the three cell lines studied are summarized in Figs. 7 and 8.

Compared to control cells, depletion of UCK2 protein reduced 2′-MeC phosphorylation by about 5-fold in HeLa (Fig. 7A) and Huh7 (Fig. 8A) cells, and 3-fold in HepG2 cells (Fig. 7B). In contrast, UCK2 depletion did not reduce the phosphorylation of 2′-F-2′-MeC in these cell lines (Figs. 7C and 8B).

Next the impact of UCK1 depletion was determined. For 2′-MeC, UCK1 depletion had little or no effect in HeLa (Fig. 7A), HepG2 (Fig. 7B) or Huh7 cells (Fig. 8A). Similarly, UCK1 knockdown did not have a significant effect on 2′-F-2′-MeC phosphorylation as seen in Figs. 7C and 8B.

For dCK, the effect of depletion on 2′-MeC phosphorylation was found to be minimal (<20% reduction) after 48 h in Huh7 (Fig. 8A) and HepG2 cells (data not shown); HeLa cells are less relevant to the antiviral activity of 2′-MeC and were not tested in this assay. In contrast, 2′-F-2′-MeC phosphorylation was reduced by ~75% in dCK-silenced Huh7 cells (Fig. 8B). Although this accords well with the approximately 80% reduction of dCK protein levels estimated by Western blot analysis, we further validated this result by measuring the enzymatic dCK activity present in a portion of the cell lysates using an assay based on the phosphorylation of CdA, a substrate that is specific for dCK. Compared to control lysates, the lysates from the silenced cells contained about 5-fold less dCK activity (data not shown).

Taken together, the preceding results provide strong support for the idea that, at least in cell culture, dCK is the primary enzyme driving the initial phosphorylation of 2′-F-2′-MeC (Murakami et al., 2007), whereas UCK2 is the key enzyme behind 2′-MeC phosphorylation. Less clear from the data is whether any role is left for dCK in the intracellular phosphorylation of 2′-MeC. Since silencing is typically less than 100% efficient it is likely that much or all of the residual 2′-MeC phosphorylation (20–40%) seen in the different cell types simply reflects the remaining levels of UCK2. However, given the limitations of the silencing methodology coupled with the inherent variability of these complex cell-based assays, we cannot completely exclude the possibility that dCK may make a minor contribution to the overall phosphorylation of 2′-MeC in the tested cell lines.

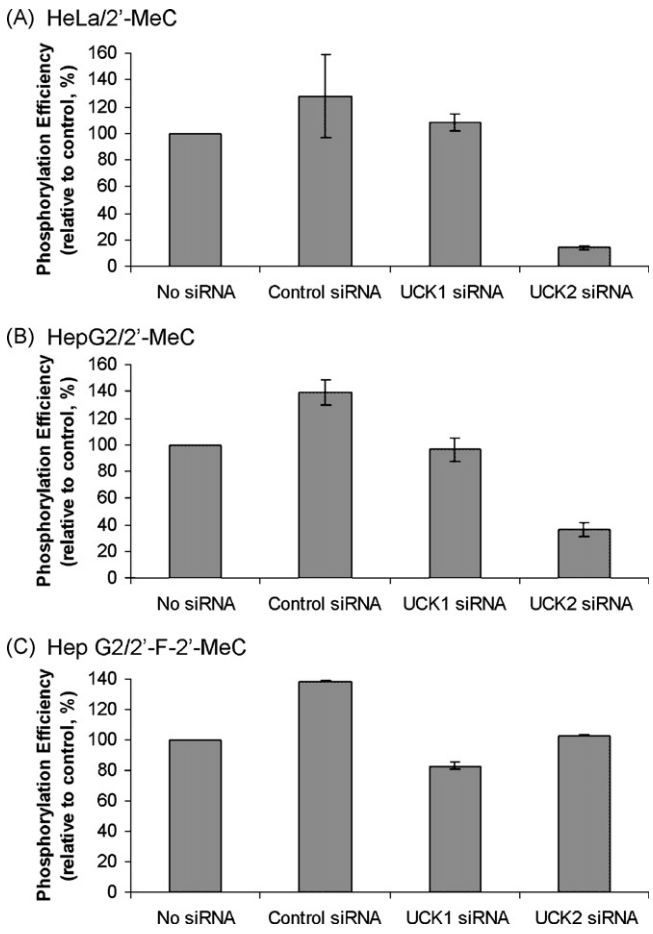

Fig. 7. Effects of siRNA treatment on the phosphorylation of 2′-MeC in HeLa (A) and HepG2 (B) cells and 2′-F-2′-MeC in HepG2 cells (C). Data reflect means and standard deviations obtained from five (A) or two (B, C) independent experiments.

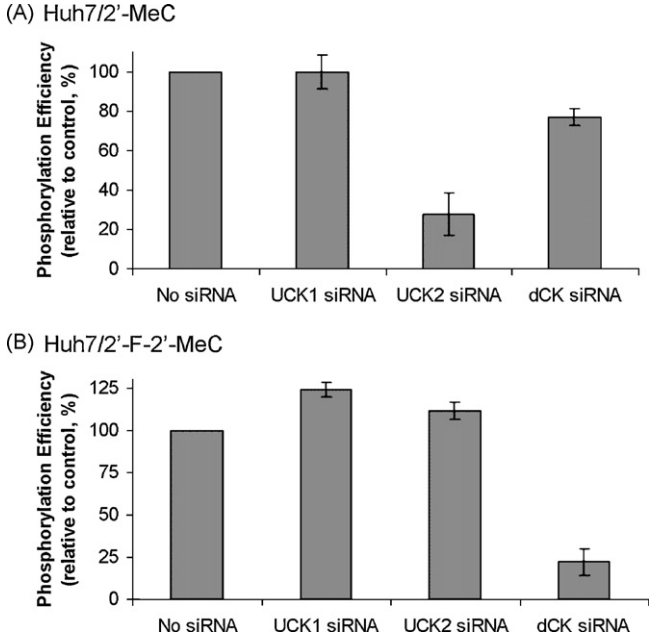

Fig. 8. Effects of siRNA treatment on the phosphorylation of 2′-MeC (A) and 2′-F-2′-MeC (B) in Huh7 cells. Data reflect means and standard deviations obtained from six (A) or three (B) independent experiments.

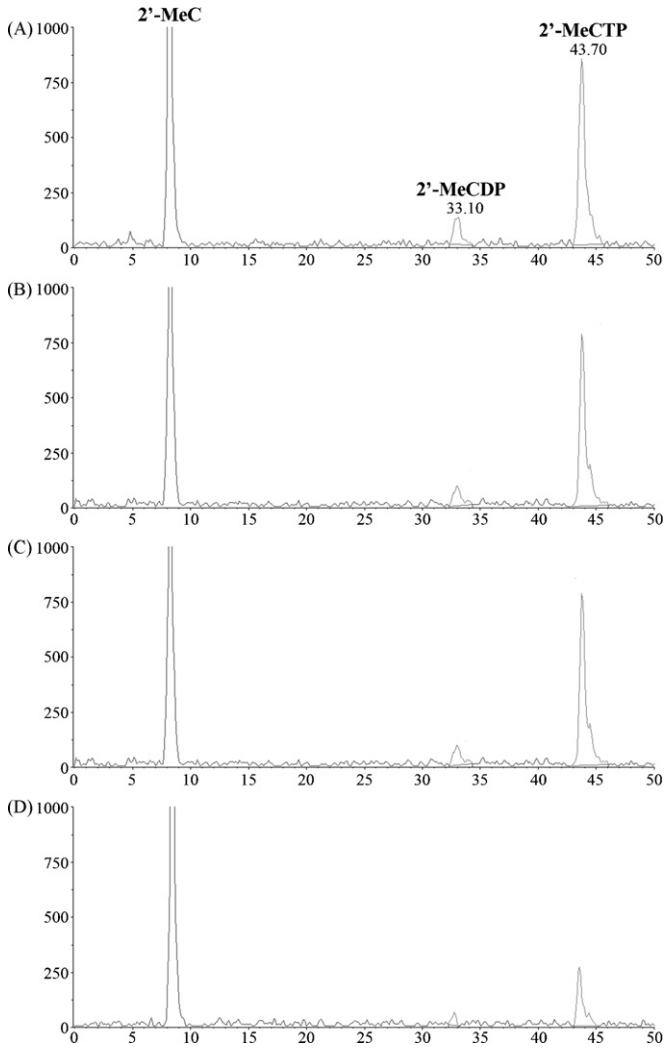

Fig. 9. HPLC analysis detected phosphorylated 2′-MeC species in control Huh7 cells (A); and in cells 48 h after transfection with siRNAs specific for UCK1 (B), dCK (C), or UCK2 (D).

3.5. The effect of silencing on the phosphorylation profile of 2′-MeC in cells

The HPLC chromatogram shown in Fig. 9A depicts the profile of 2′-MeC species metabolized in control Huh7 cell treated with 10 μM radioactive 2′-MeC for 24 h (Fig. 9A). Also shown is the impact of silencing with siRNAs specific for UCK1 (Fig. 9B), dCK (Fig. 9C) or UCK2 (Fig. 9D). Similar results were obtained in HepG2 cells (data not shown).

As can be seen from the chromatographic profiles, exposure of cells to radioactive 2′-MeC resulted mainly in the formation of the corresponding triphosphate product. Only a low amount of 2′-MeCDP and no 2′-MeCMP was found under these conditions. The predominance of 2′-MeCTP product coupled with the lack of accumulation of the MP and DP intermediates is consistent with the idea that the 2′-MeCMP intermediate, once formed, is rapidly and efficiently converted to 2′-MeCTP. Thus, the first 2′-MeC phosphorylation step appears to be the rate-limiting step in 2′-MeCTP production, at least in the cell systems studied in this report.

A significant decrease in the amount of 2′-MeCTP end product was seen only in cells transected with UCK2-specific siRNA (Fig. 9D), indicating that a decrease in UCK2-mediated production 2′-MeCMP leads directly to a decrease in the TP active species. As expected, no change in 2′-MeCTP levels was seen in cells transfected with the other two siRNA species.

No deamination of 2′-MeC or its phosphorylated metabolites to the corresponding uridine derivatives (e.g. 2′-MeU or 2′-MeUMP) was seen in any cell type in this study. In our experience it takes a longer time to generate these uridine species. Thus, low and variable amounts (less then 4.5%) of 2′-MeUTP were found only in HepG2 cells after 48 h incubation with ^{3}H-2′-MeC (data not shown).

4. Discussion

The main goal of this study was to identify the human kinase(s) responsible for the conversion of 2′-MeC to its 5′-monophosphate metabolite, 2′-MeCMP. This is the first phosphorylation step in the pathway leading to the production of the 2′-MeC triphosphate active species that is responsible for inhibiting the HCV polymerase. Data presented in this paper are consistent with the idea that the first phosphorylation step for 2′-MeC is a rate-limiting step that may restrict the antiviral activity of this agent in man. This limitation, which likely applies to all the cytidine analogs currently in clinical development for the treatment of HCV, may be overcome to some extent by the use of high doses of nucleoside analogs, leading to increased triphosphate production in the liver. However, high doses of nucleoside analogs may also result in an increase in the off-target toxicities and side effects encountered with these agents.

Two groups have reported different kinases responsible for 2′-MeC phosphorylation. Klumpp et al. (2008) found that dCK did not phosphorylate 2′-MeC but UCK1 did. Murakami et al. (2007) found that UCK1 did not phosphorylate 2′-MeC whereas dCK did, although with low efficiency.

Our study attempted to resolve this discrepancy using two different approaches: by testing 2′-MeC phosphorylation with purified kinases and by investigating the impact of silencing the specific kinase expression (by siRNA technique) on phosphorylation of 2′-MeC.

We first evaluated the ability of recombinant UCK1, UCK2, and dCK to phosphorylate 2′-MeC and several control nucleoside analogs in vitro. While recombinant UCK2 and dCK were both able to phosphorylate 2′-MeC in vitro, albeit with much less efficiency than their natural substrates, UCK1 did not phosphorylate 2′-MeC at all, consistent with reports that this enzyme has a relatively narrow substrate specificity (Van Rompay et al., 2001; Murakami et al., 2007). Our biochemical results showing that dCK, but not UCK1, can phosphorylate 2′-MeC generally agree with those of Murakami et al. (2007) and contradict Klumpp et al. (2008). More importantly, however, we also showed that UCK2 can catalyze this reaction. In contrast to 2′-MeC, the closely related cytidine analog 2′-F-2′-MeC was a substrate for dCK but not for the two UCK enzymes. This finding confirms a prior report (Murakami et al., 2007) that 2′-F-2′-MeC is phosphorylated by dCK and suggests that 2′-F-2′-MeC behaves more like a deoxynucleoside than a ribonucleoside due to the presence of the 2′-fluoro group.

While our biochemical data suggested that both UCK2 and dCK could potentially be responsible for converting 2′-MeC to 2′-MeCMP, a series of carefully controlled silencing experiments using gene-specific siRNAs pinpointed UCK2 as the key enzyme responsible for the monophosphorylation of 2′-MeC, at least in the three different human cell lines tested in this study. Thus, reduction of UCK2 levels decreased 2′-MeC phosphorylation by 70–80% in all three human cell lines tested. In contrast, dCK appeared to be responsible for no more than 20% of 2′-MeC phosphorylation in Huh7 and HepG2 cells: this low value lies within the expected range of variability for a complex cell-based assay. Given this and the fact that our UCK2 silencing experiments almost certainly did not achieve a 100% protein depletion, we cannot conclude with

certainty that dCK has any role in the in vitro phosphorylation of 2′-MeC in cells. However, we do not exclude a minor role for this enzyme.

In other respects, the siRNA results correlated well with those obtained with the recombinant kinases and further validated the biochemical findings. Thus, siRNA silencing ruled out a role for the UCK1 kinase in the phosphorylation of 2′-MeC in the three human cells lines. In addition to confirming the work of Murakami et al. (2007) by showing that phosphorylation of 2′-F-2′-MeC is mediated by dCK, our silencing experiments further rule out the involvement of UCK1 or UCK2 in this process. Importantly, these results clearly demonstrate that dCK is functional in the test cell types, thereby establishing that the phosphorylation of 2′-MeC by UCK2 rather than dCK is not simply due to a lack of a functional dCK kinase in these cells.

The idea that a UCK enzyme is responsible for 2′-MeC phosphorylation in cultured cells was first demonstrated by substrate competition studies showing that the intracellular phosphorylation of 2′-MeC to 2′-MeC triphosphate was reduced in a dose-dependent fashion in the presence of cytidine ($EC_{50} = 19.17 \pm 4.67\ \mu M$) or uridine ($EC_{50} = 20.92 \pm 7.10\ \mu M$), but not deoxycytidine ($EC_{50} > 100\ \mu M$) (E. Cretton-Scott, data not shown). The present work now extends these in vitro competition experiments by demonstrating that UCK2, and not UCK1, is the enzyme responsible for the initial phosphorylation of 2′-MeC in cell culture.

Our study demonstrates the importance of using cell-based systems to confirm results obtained on the phosphorylation of nucleoside analogs by purified enzyme. As noted above, dCK was shown to be fully functional in the cultured test cells but appeared to play at best a minor role or perhaps even no role in the phosphorylation of 2′-MeC in cells. While the basis for the differences in results between the two biochemical and cell-based systems remains unknown, a variety of factors, such as intracellular enzyme levels or activity, competition with the natural substrates, the existence of feedback mechanisms, the presence of specific natural products within the cell, or the possibility that specific kinases may function in multi-protein enzymatic complexes may lead to differences between the two systems.

Our findings define UCK2 as the key kinase involved in the formation of 2′-MeC monophosphate from 2′-MeC in cultured human cells. Since the HCV replicon-containing Huh7 cell line is widely used in HCV drug discovery and has been successfully used to predict which nucleosides will be active in HCV patients, we felt it was very important to identify kinases responsible for activation of 2′-MeC in this key cell line.

Although among normal human tissues UCK2 expression was observed only in placenta (Van Rompay et al., 2001), it should be noted that very little is known about the expression of UCK1, UCK2 or dCK in primary human hepatocyte cultures or in vivo in the context of the uninfected or HCV-infected liver. It remains formally possible that the phosphorylation pathways used in hepatocytes or tissues are different from those defined in cultured cells. However, phosphorylation studies have shown that cytidine analogs such as 2′-MeC, 2′-F-2′-MeC, and 4′-azidoC are phosphorylated to about the same limited extent (around 20 pmol of phosphorylated nucleoside species per million cells) in primary hepatocytes from rat, monkey or human as they are in cultured human cell lines (Cretton-Scott et al., 2008; Standring et al., 2008; Cretton-Scott, unpublished results). This suggests that the same restrictive first phosphorylation steps are operative in these different systems. Conducting more study in human hepatocytes especially in HCV-infected hepatocytes, will further clarify this question.

The preceding observations suggest the possibility of devising strategies to improve the antiviral activity of the nucleoside which are inefficiently phosphorylated in the initial kinase step. In particular the use of monophosphorylated nucleotide prodrugs provides a potential approach to bypass the first kinase step, thereby leading to increased levels of the triphosphate active species and hence potentially increased antiviral activity in the clinic compared to a corresponding nucleoside analog.

Acknowledgments

We thank Jesse Potash (ProSanos Corporation) and Valérie Philippon (former employee of Idenix Pharmaceuticals) for assistance with manuscript preparation. We also thank our colleagues John Bilello, Ben Mayes and Joseph McCarville for helpful comments.

References

Ahmed, N.K., 1981. Determination of pyrimidine phosphoribosyltransferase and uridine kinase activities by an assay with DEAE-paper discs. J. Biochem. Biophys. Methods 4, 123–130.

Ali, S., Leveque, V., Le Pogam, S., Ma, H., Philipp, F., Inocencio, N., Smith, M., Alker, A., Kang, H., Najera, I., Klumpp, K., Symons, J., Cammack, N., Jiang, W.-R., 2008. Selected replicon variants with low-level in vitro resistance to the hepatitis C virus NS5B polymerase inhibitor PSI-6130 lack cross-resistance with R1479. Antimicrob. Agents Chemother. 52, 4356–4369.

Anderson, E.P., Brockman, R.W., 1964. Feedback inhibition of uridine kinase by cytidine triphosphate and uridine triphosphate. Biochim. Biophys. Acta 91, 380–386.

Arner, E.S., Spasokoukotskaja, T., Eriksson, S., 1992. Selective assays for thymidine kinase 1 and 2 and deoxycytidine kinase and their activities in extracts from human cells and tissues. Biochem. Biophys. Res. Commun. 188, 712–718.

Beauséjour, C.M., Gagnon, J., Primeau, M., Momparler, R.L., 2002. Cytotoxic activity of 2′,2′-difluorodeoxycytidine, 5-aza-2′-deoxycytidine and cytosine arabinoside in cells transduced with deoxycytidine kinase gene. Biochem. Biophys. Res. Commun. 293, 1478–1484.

Cooper, C., Lawitz, E.J., Ghali, P., Rodriguez-Torres, M., Anderson, F.H., Lee, S.S., Proulx, L., 2007. Antiviral activity of the non-nucleoside polymerase inhibitor, VCH-759, in chronic hepatitis C patients: results from a randomized, double-blind, placebo-controlled, ascending multiple dose study. Hepatology 46 (Suppl. 1), 864A.

Cretton-Scott, E., Perigaud, C., Peyrottes, S., Licklider, L., Camire, M., Larsson, M., La Colla, M., Hildebrand, E., Lallos, L., Bilello, J., McCarville, J., Seifer, M., Liuzzi, M., Pierra, C., Badaroux, E., Gosselin, G., Surleraux, D., Standring, D.N., 2008. In vitro antiviral activity and pharmacology of IDX184, a novel and potent inhibitor of HCV replication. J. Hepatol. 48, S220.

De Francesco, R., Carfí, A., 2007. Advances in the development of new therapeutic agents targeting the NS3-4A serine protease or the NS5B RNA-dependent RNA polymerase of the hepatitis C. Adv. Drug Deliv. Rev. 59, 1242–1262.

Ives, D.H., Durham, J.P., Tucker, V.S., 1969. Rapid determination of nucleoside kinase and nucleotidase activities with tritium-labeled substrates. Anal. Biochem. 28, 192–205.

Johansson, M., Brismar, S., Karlsson, A., 1997. Human deoxycytidine kinase is located in the cell nucleus. Proc. Natl. Acad. Sci. 94, 11941–11945.

Klumpp, K., Kalayanov, G., Ma, H., Le Pogam, S., Leveque, V., Jiang, W.-R., Inocencio, N., De Witte, A., Rajyaguru, S., Tai, E., Chanda, S., Irwin, M.R., Sund, C., Winqist, A., Maltseva, T., Eriksson, S., Usiva, E., Smith, M., Alker, A., Najera, I., Cammack, N., Martin, J.A., Johansson, N.G., Smith, D.B., 2008. 2′-Deoxy-4′-azido nucleoside analogs are highly potent inhibitors of Hepatitis C virus replication despite the lack of 2′-alfa-hydroxyl groups. J. Biol. Chem. 283, 2167–2175.

Le Pogam, S., Seshaadri, A., Kosaka, A., Hu, S., Kang, H., Symons, J., Klumpp, K., Cammack, N., Najera, I., 2008. A high barrier to resistance may contribute to the robust antiviral effect demonstrated by R1626 in HCV genotype 1-infected treatment-naive patients. Hepatology 46, 813A.

Lalezari, J., Gane, E., Rodriguez-Torres, M., DeJesus, E., Nelson, D., Everson, G., Jacobson, I., Reddy, R., Hill, G.Z., Beard, A., Symonds, W.T., Berrey, M.M., McHutchison, J.G., 2008. Potent antiviral activity of the HCV nucleoside polymerase inhibitor R7128 with PEG-IFN and ribavirin: interim results of R7128 500 mg BID for 28 days. J. Hepatol. 48, S29.

Liu, Y., Jiang, W.W., Pratt, J., Rockeway, T., Harris, K., Vasavanonda, S., Tripathi, R., Pithawalla, R., Kati, W.M., 2006. Mechanistic study of HCV polymerase inhibitors in individual steps of the polymerization reaction. Biochemistry 45, 11312–11323.

Meanwell, N.A., Koszalka, G.W., 2008. 2007: a difficult year for HCV drug development. Curr. Opin. Investig. Drugs 9, 128–131.

Murakami, E., Bao, H., Ramesh, M., McBrayer, T.R., Whitaker, T., Micolochick Steuer, H.M., Schinazi, R.F., Stuyver, L.J., Obikhod, A., Otto, M.J., Furman, P.A., 2007. Mechanism of activation of β-D-2′-deoxy-2′-fluoro-2′-C-methylcytidine and inhibition of hepatitis C virus NS5B RNA polymerase. Antimicrob. Agents Chemother. 51, 503–509.

Nelson, D., Pockros, P., Godofsky, E., Rodriguez-Torres, M., Everson, G., Fried, M., Ghalib, R., Harrison, S., Nyberg, L., Shiffman, M., Chan, A., Hill, G., 2008. High end-of-treatment response (84%) after 4 weeks of R1626, peginterferon alfa-2A (40KD) and ribavirin followed by a further 44 weeks of peginterferon alfa-2A and ribavirin. J. Hepatol. 48, S371.

Pawlotsky, J.M., Chevaliez, S., McHutchison, J.G., 2007. The hepatitis C virus life cycle as a target for new antiviral therapies. Gastroenterology 132, 1979–1998.

Poordad, F., Lawitz, E.J., Gitlin, N., Rodriguez-Torres, M., Box, T., Nguyen, T., Pietropaolo, K., Liu, W., Fielman, B., Mayers, D., 2007. Efficacy and safety of valopicitabine in combination with pegylated interferon-a (PEG-IFN) and ribavirin (RBV) in patients with chronic hepatitis C. Hepatology 46, 866A.

Reddy, R., Rodriguez-Torres, M., Gane, E., Robson, R., Lalezari, J., Everson, G.T., DeJesus, E., McHutchison, J.G., Vargas, H.E., Beard, A., Rodriguez, C.A., Hill, G.Z., Symonds, W., Berrey, M., 2007. Antiviral activity, pharmacokinetics, safety, and tolerability of R7128, a novel nucleoside HCV polymerase inhibitor, following multiple, ascending, oral doses in patients with HCV genotype 1 infection who have failed prior therapy. Hepatology 46, 232A.

Roy, B., Verri, A., Lossani, A., Spadari, S., Focher, F., Aubertin, A.-M., Gosselin, G., Mathe, C., Perigaud, C., 2004. Enantioselectivity of ribonucleotide reductase: a first study using stereoisomers of pyrimidine 2′-azido-2′-deoxynucleosides. Biochem. Pharmacol. 68, 711–718.

Shafiee, M., Griffon, J.-F., Gosselin, G., Cambi, A., Vincenzetti, S., Vita, A., Eriksson, S., Imbache, J.-L., Maury, G., 1998. A comparison of the enantioselectivities of human deoxycytidine kinase and human cytidine deaminase. Biochem. Pharmacol. 56, 1237–1242.

Sabini, E., Ort, S., Monnerjahn, C., Konrad, M., Lavie, A., 2003. Structure of human dCK suggests strategies to improve anticancer and antiviral therapy. Nat. Struct. Biol. 10, 513–519.

Shimamoto, Y., Koizumi, K., Okabe, H., Kazuno, H., Murakami, Y., Nakagawa, F., Matsuda, A., Sasaki, T., Fukushima, M., 2002. Sensitivity of human cancer cells to the new anticancer ribo-nucleoside TAS-106 is correlated with expression of uridine-cytidine kinase 2. Jpn. J. Cancer Res. 93, 825–833.

Standring, D.N., Lanford, R., Wright, T., Chung, R.T., Bichko, V., Cretton-Scott, E., Pan-Zhou, X., Bergelson, S., Qu, L., Tausek, M., Bridges, E., Moussa, A., Storer, R., Pierra, C., Benzaria, S., Gosselin, G., La Colla, P., Sommadossi, J.P., 2003. NM 283 has potent antiviral activity against genotype 1 chronic hepatitis C virus (HCV-1) infection in the chimpanzee. J. Hepatol. 38, 3.

Standring, D.N., Lanford, R., Cretton-Scott, E., Licklider, L., Larsson, M., Pierra, C., Gosselin, G., Perigaud, C., Surleraux, D., Mayes, B., Moussa, A., Selden, J., 2008. Potent antiviral activity of second generation nucleoside inhibitors, IDX102 and IDX184, in HCV-infected chimpanzees. J. Hepatol. 48, S30.

Usova, E., Maltseva, T., Foldesi, A., Chattopadhayaya, J., Eriksson, S., 2004. Human deoxycytidine kinase as a deoxyribonucleoside phosphorylase. J. Mol. Biol. 344, 1347–1358.

Van Rompay, A.R., Norda, A., Lindén, K., Johansson, M., Karlsson, A., 2001. Phosphorylation of uridine and cytidine nucleoside analogs by two human uridine–cytidine kinases. Mol. Pharmacol. 59, 1181–1186.

Van Rompay, A.R., Johansson, M., Karlsson, A., 2003. Substrate specificity and phosphorylation of antiviral and anticancer nucleoside analogues by human deoxyribonucleoside kinases and ribonucleoside kinases. Pharmacol. Ther. 100, 119–139.